Lafia Journal of Scientific & Industrial Research (LJSIR), Vol. 3(2), 2025
p-ISSN: 3026 – 9288 e-ISSN: 3027 – 1800 pages: 59 – 70
https://lafiascijournals.org.ng/index.php/ljsir/index ⇒ Published by the Faculty of Science,
Federal University of Lafia, Nasarawa State, Nigeria

Groundwater Potential and its Suitability for Drinking and Irrigation Purposes in Federal University of Lafia, Nasarawa State, North-Central Nigeria

Nuhu Degree Umar[1], Andarawus Yohanna[1]*, Ahmad Ibrahim Aliyu[1], Abdulhakim Suleiman Usman[1], Salihu Aliyu[1], Safiyanu Tanko Musa[2] & Muhammad Sanusi Idris[1]
[1]Department of Geology, Federal University of Lafia, PMB 146, Nasarawa State, Nigeria
[2]Department of Chemistry, Federal University of Lafia, PMB 146, Nasarawa State, Nigeria

Abstract

This study assessed the groundwater potential and its suitability for drinking and irrigation purposes at the Federal University of Lafia, Nasarawa State, Northcentral Nigeria. Vertical electrical sounding (VES) using Schlumberger electrode array with a maximum half-current electrode separation of 200 m was employed. Interpretation of the VES results showed that the area is characterized by 4–5 geo-electric subsurface layers, viz. topsoil/laterite, sandy shale, shale and sandstone. From the geo-electric curves simulated, the curve type varies from KH-type (11.3%), QH-type (44.4%), H-type (22.2%), and Q-type (22.2%). The resistivity values ranged from 1.28 to 2792 Ωm. Low resistivity values were associated with shale; moderate resistivity values were associated with topsoil and high resistivity values with sandstone. Fifteen groundwater samples were collected from boreholes and analysed for major anions and cations. The water quality index (WQI) was evaluated from physicochemical parameters and used in assessing the groundwater quality for drinking, while the electrical conductivity (EC), percentage sodium (%Na), sodium absorption ratio (SAR) and magnesium hardness (MH) were evaluated to assess its suitability for irrigation. Most of the parameters have low concentrations and are indicative of natural processes such as water–rock interactions controlling the chemistry of groundwater in the area except nitrate. Three water types: calcium bicarbonates, calcium sulfate and sodium chloride waters were revealed, which implied that cation exchange controls the groundwater quality in the area. Based on sodium adsorption ratio, magnesium adsorption ratio, Kelly's ratio, and chloro-alkaline indices, the groundwater in the area is good for irrigation purposes.

Keywords: Groundwater, Resistivity, Water Quality Index, Kelly Ratio, Irrigation

Article History

Submitted
May 13, 2025

Revised
June 28, 2025

First Published Online
July 06, 2025

Correspondences
A. Yohanna ✉
yohana.andarawus@science.fulafia.edu.ng

doi.org/10.62050/ljsir2025.v3n2.538

Introduction

In spite of the seasonal supply of surface waters through the existing rivers, streams and rivulets, humans suffer from many shortages in surface water quantities. Pressure on global water resources is increasing in an unprecedented manner. In Nigeria, groundwater accounts for over 80% of the domestic water supply largely due to its lower cost of development and probably because of its proximity to the final consumers [1]. Groundwater, therefore, continues to play a significant role as a source of potable water for many uses in the institutional, domestic, agricultural, and industrial sectors, especially in places where municipal water systems are progressively failing. About one-third of the world's water supply comes from groundwater, making it the most abundant and cleanest source of water on Earth [2]. However, the demand for potable fresh water is increasing due to global population growth, urbanization, and climate change impacts, putting tremendous pressure on existing groundwater reserves. Clean drinking water is a basic human need, and its deficiency or contamination can have major detrimental impacts on public health, ranging from illness to epidemics. Humans primarily obtain their water from lakes, streams, and rain. However, due to pollution and contamination caused by human and industrial activities, some sources of drinking water are unfit for human consumption [2].

Various geophysical techniques have been employed to identify potential water-bearing zones. Nonetheless, the electrical resistivity method is believed to have the most accurate portability, intuitiveness, and depth of penetration. The fundamentally significant resistivity comparison between worn and/or fissured columns and highly resistive fresh bedrock determines the technique's suitability. The weathered and fractured layers are most likely to contain groundwater [2, 3]. The demand for water in the Federal University of Lafia campus is on the rise due to the growing population and infrastructure. Several studies, carried out on a regional scale, have provided

valuable insights into the hydrogeological regimes and groundwater quality of the Middle Benue Trough [4, 5]. However, these studies have often fallen short of providing comprehensive data on the groundwater potential of the area under investigation.

This study uses the electrical resistivity method to investigate the groundwater potential of the Federal University of Lafia. In addition, the physiochemical assessment of groundwater samples was carried out in order to determine their suitability for various uses. The study will serve as a foundation for future field investigations, as well as continuous evaluations and monitoring of groundwater sources.

Study area description

The study area covers approximately 4 km^2, bounded by latitudes 8° 24' 00"N to 8° 29' 48"N and longitudes 8° 32' 30"E to 8° 34' 59"E (Fig. 1). The area enjoys excellent accessibility, facilitated by the Lafia-Awe and Lafia - Makurdi roads. The topography is generally low-undulating, drained by the River Amber and its tributaries, giving the area a dendritic drainage pattern. Wet and dry seasons are typical climatic conditions in the area. The wet season begins in April and lasts around October and November, while the dry season commences in October and lasts until late April. The research area experiences 1000-500 mm of annual rainfall on average, along with 70% mean humidity and 60–80% relative humidity. Consistently high temperatures year-round are prominent due to its tropical savanna climate, with an average yearly temperature of between 27 and 30°C. March and May are usually the hottest months, when temperatures frequently soar above 30°C [6]. Dispersed trees, shrubs, and grasses make up the vegetation, which is typical of the tropical Guinea savanna.

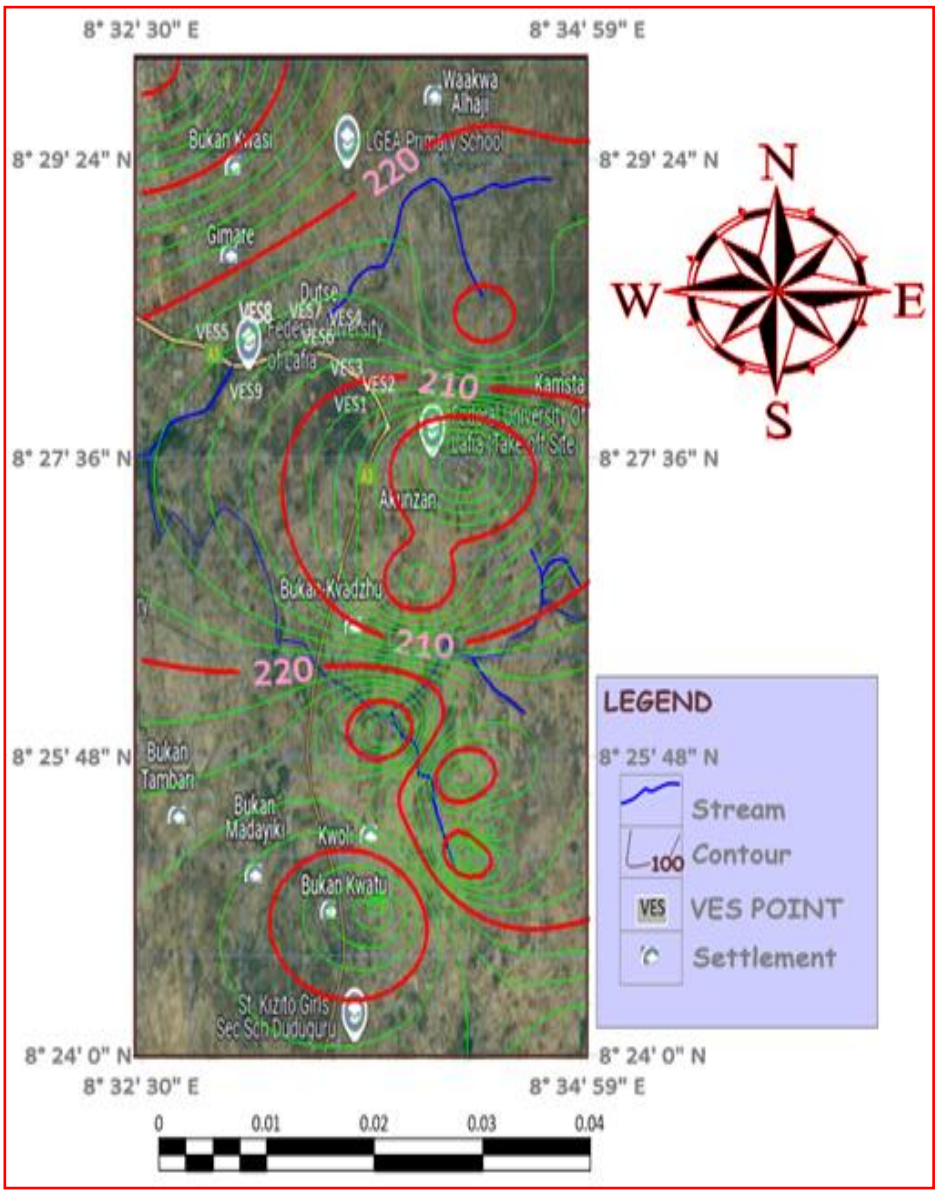

Figure 1: Satellite imagery map of the study area showing VES points

Regional geology of the area

The Benue Trough is an extensive rift basin formed during the Late Jurassic to Early Cretaceous periods [7]. According to some researchers [7, 8], it is an elongate linear intra-cratonic mega-shear structure that runs NNE-SSW and is about 800 km long and 150 km wide. The southern and northern ends of it are the northern and southern boundaries of the Niger Delta and Chad Basins, respectively. During the mid-Santonian epoch, the Benue Trough experienced a significant tectonic event that had a tremendous effect on the entire basin and resulted in extensive uplift, compressional folding, and faulting [7]. As a result, more than 100 anticlines and synclines were formed, notably the Giza anticline and Obi syncline in the Middle Benue Trough; the Lamurde anticline and Dadiya syncline in the Upper Benue Trough; and the Abakaliki anticlinorium and Afikpo syncline in the Lower Benue Trough [7].

The Benue Trough is made up of multiple pull-apart sub-basins that trend NE-SW, separated into lower, middle, and upper portions. These sub-basins are filled with Cretaceous to Tertiary sediments that experienced substantial structural deformation prior to the mid-Santonian period [7]. The Middle Benue Trough is divided into six litho-stratigraphic successions, comprising the Asu River Group, Awe Formation, Keana Formation, Ezeaku Formation, Awgu Formation, and Lafia Formation. The Albian-oldest-basal Asu River Group, deposited during the Mid-Albian marine transgression of the South Atlantic Gulf of Guinea, directly overlies the basement unconformably. It consists of the Arufu limestone, the Uomba Formation, and the Gboko limestone. Lithologically, the group comprises limestones, shales, calcareous shales, micaceous siltstones, mudstones, and clays. The Late Albian to Early Cenomanian Awe Formation, which overlies the Asu River Group, is characterized by transitional marine to fluvial sediments comprising whitish, medium- to fine-grained flaggy sandstones, claystones, and carbonaceous shales [7, 8]. The Keana Formation, unconformably overlying the Awe Formation, is a product of Cenomanian regression that resulted in the deposition of fluviodeltaic sediments. This formation consists of coarse-grained sandstones with notable cross-bedding and feldsparthic makeup, alternating layers of limestone and shales, and conglomerates with an occasional appearance [7, 8].

The Ezeaku Formation overlies the Keana Formation, consisting of shaly limestones, medium- to fine-grained micaceous sandstones, and calcareous shales deposited during early marine transgression in the Late Cenomanian. The Late Turonian-Coniacian Awgu Formation is said to conformably overlie the Ezeaku Formation. This coal-bearing formation, marking the end of marine sedimentation in the Middle Benue Trough, is characterized by carbonaceous shales that are fissile in nature [7]. The youngest Lafia Formation, deposited during the Maastrichtian, unconformably overlaid the Awgu Formation. It is notably characterized by intense ferruginization and is lithologically composed of continental sediments ranging from sandstones, siltstones, claystones, and mottled clays [7, 8].

Geology and hydrogeology of the area

The study area is underlain by Late Turonian-Early Santonian sediments of the Awgu Formation within the Middle Benue Trough.Lithologically the area is made up of ferruginous siltstone, ferruginious sandstone and shale (Fig. 2). Shale is the dominant lithology, covering about 95% of the area. The shale is divided into two lithofacies: grey shale and carbonaceous shale. The grey shale is fine-grained, with a smooth texture dominated by shiny micas. It is fissile and feels smooth to the touch; however, the presence of finely dispersed silty materials gives it a slightly gritty texture. A notable reddish coloration was observed between the faint fissile layers, suggesting the presence and oxidation of iron oxide and other iron-bearing minerals. It also indicates localized changes in post-depositional processes within the shale. The carbonaceous shale appears dark grey, indicative of the presence of organic matter. It is fine-grained, fissile, and more friable than the grey shale [9].

The Middle Benue has considerable hydrogeological challenges due to the nature of its prospective aquifers. The aquifers are generally restricted in size, thinly developed with persistent clay and shale interbedding that are less porous and permeable, or, in some cases, highly indurated in nature that only allow passage through secondary voids generated by fractures and joints. The Awgu Formation comprises carbonaceous and calcareous shales, occasionally interspersed with limestone, and a medium- to coarse-grained, permeable, water-bearing sandstone layer. However, the limited thickness and lateral extent of the sandstone reduce the overall groundwater potential of Awgu Formation [9].

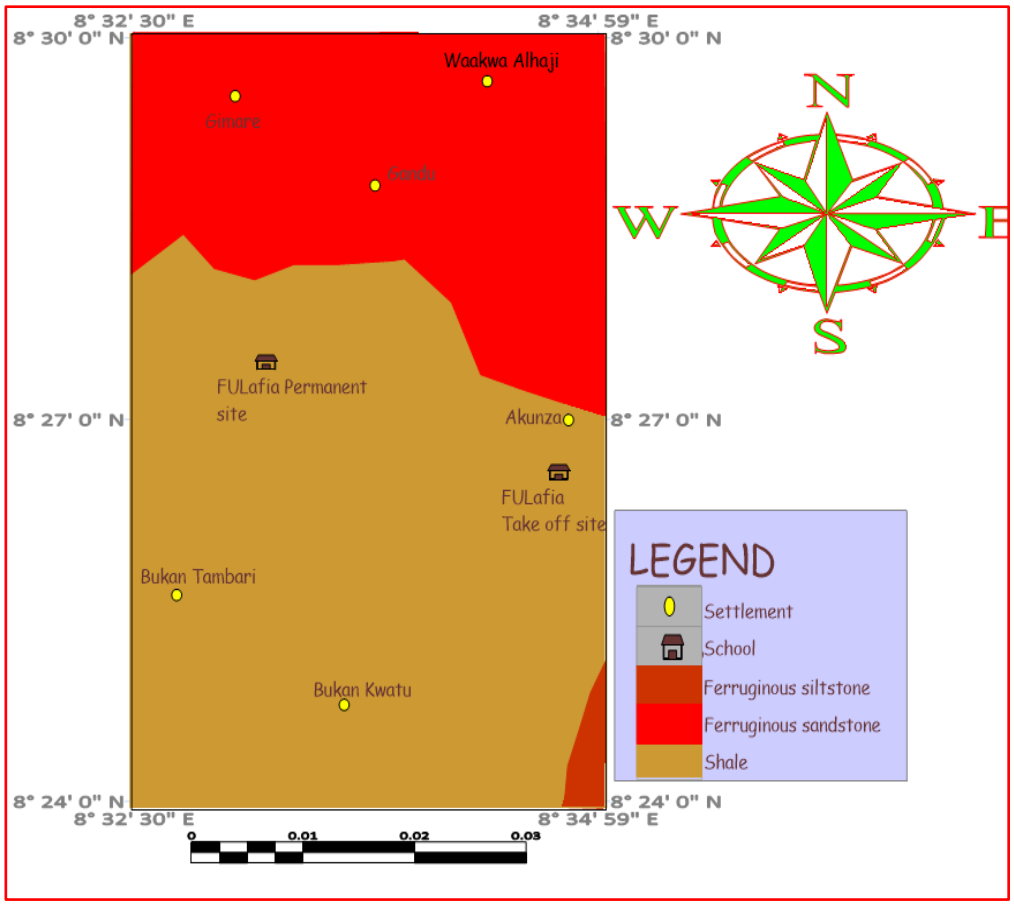

Figure 2: Geological Map of the Study Area

Materials and Method

Static water level measurements

The static water levels (SWLs) and depths of 14 boreholes were determined using dip meter (the dipper-T model). The topography and coordinates (latitude and longitude) of each location were determined using the Global Positioning System (GPS) (e-Trex 20 Garmin model). Sampling was done early in the morning before water abstraction for the day.

The SWL and topographic elevation above mean sea level values were used to estimate the hydraulic head of each well. The Surfer 13 program was used to generate a hydraulic head map based on these values. To show the direction of groundwater flow in the area, angled piezometric lines were constructed [10].

Geophysical data acquisition

Subsurface investigation was conducted using ABEM SAS 1000 Terameter. Vertical electrical sounding (VES) technique employing the Schlumberger electrode configuration was used for data acquisition. This involves the injection of measured low frequency direct current (DC) into the subsurface via a pair of current electrodes (AB) and measuring the corresponding voltage drop via another pair of potential electrodes (MN). Vertical electrical sounding (VES) is carried out by extending the electrode system (four electrodes) on a straight line, to produce vertical changes in the electrical resistivity of the subsurface, relative to the various strata encountered (Fig. 3).

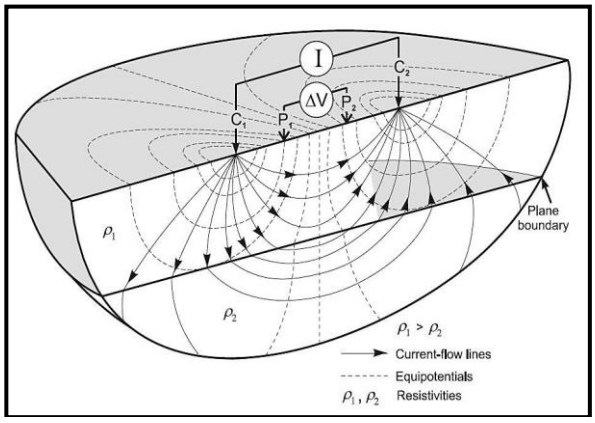

Figure 3: Principle of resistivity measurement with a four-electrode array [11]

The depth of penetration is proportional to the separation between the current electrodes in homogeneous subsurface and varying the electrodes separation, provides information about the stratification of the subsurface [1, 10–14]. Current electrode spacing (AB/2) varied from 1 to 400 m, while potential electrode separation was varied between 0.5 and 25 m. The apparent resistivity was computed using [12]:

$$\rho a = \pi . \left[\frac{(AB/2) - (MN/2}{MN} \right] . R \qquad (1)$$

Where: ρa is the apparent resistivity; AB is the distance between the two current electrodes; MN is the distance between the potential electrodes; R is the electrical resistance measured

Each apparent resistivity value computed from the above equation was plotted on a log-log graph to the corresponding current electrode spacing, from which the layers resistivities, depths, thicknesses and curve types were deduced. The conventional quantitative interpretation using partial curve matching was done by matching the field curves with the auxiliary curves. Computer modelling software IPI2win was used in the inversion and iteration of each VES point from which the resistivities and thicknesses of the layers determined.

Hydrogeochemical study of the area

Fifteen (15) groundwater samples were collected from boreholes in October and November 2024, using 250 mL preconditioned high-density polyethylene bottles. Bottles were washed with nitric acid and rinsed with distilled water. Temperature, electrical conductivity (EC), pH and total dissolved solids (TDS) measurements were conducted in situ in the field by the HACH conductivity and pH meter. Onsite testing of these variables was necessary since these parameters are likely to change during transport. Bicarbonate (HCO_3^-) titration was done at the well head using a HACH digital titrator. Sodium (Na^+) and potassium (K^{+}) were analysed using flame emission photometer (Sherwood model 420), magnesium (Mg^{2+}) and calcium (Ca^{2+}) using Varian AA240 Fast Sequential Atomic Absorption Spectrometer. Chloride (Cl^-), sulphate (SO_4^{2-}) and nitrate (NO_3^-) were analysed using ICS-90 ion chromatography at the Mohammadu Buhari Research Centre, Federal University of Lafia, Nasarawa State, Nigeria.

Weighted arithmetic water quality index (WQI) method

Water suitability for drinking was evaluated using the weighted arithmetic WQI method. The following formulas were used in this method to determine the overall WQI, relative weight, and water quality rating scale [15, 16].

$$q_i = \frac{C_i}{S_i} \times 100 \qquad (2)$$

Where qi is the weighted attribute of the element, Ci is the measured trace element concentration, and Si is the WHO (2017) standard for drinking water.

Relative weight was calculated by:

$$w_i = \frac{1}{S_i} \qquad (3)$$

Where the standard value of the i parameter is inversely proportional to the relative weight. Finally, the overall WQI was calculated according to the following expression:

$$WQI = \frac{\sum q_i w_i}{\sum w_i} \qquad (4)$$

Irrigation water quality

When evaluating an area's salinity or alkali conditions, water quality is a crucial factor [17]. Irrigation water quality is significantly influenced by the type and quantity of dissolved salts, which are primarily formed from the dissolution of rocks and soil minerals [18]. Irrigated water quality is determined by its soluble salt concentration, sodium adsorption ratio, toxic elements, and residual sodium carbonate or alkalinity [19]. Literature uses various criteria to classify groundwater for irrigation purposes, including:

1. The sodium adsorption ratio (SAR) proposed by [20] and defined as:

$$SAR = \frac{Na}{\frac{Ca+Mg}{2}} \qquad (5)$$

SAR gives an indication of the level to which irrigation water undergoes cation exchange reaction in soil.

2. Magnesium adsorption ratio (MAR) which was proposed by Raghunath [21] as:

$$MAR = \frac{Mg^{2+}}{Ca^{2+} + Mg^{2+}} \qquad (6)$$

3. Kelly's ratio defined by Kelly [22] as:

$$KR = \frac{Na^+}{Mg^{2+} + Ca^{2+}} \qquad (7)$$

4. Chloro-alkaline indices (CAI) defined as:

$$CAI = \frac{Cl^- - (Na^+ + K^+)}{Cl^-} \qquad 8$$

All ionic concentrations are in milli-equivalents per litre (meq/L) except for MAR which is expressed in percentages

Results and Discussion

Groundwater flow directions

The hydraulic head map shows regional groundwater flow from the northwestern recharge area to the northeastern part, with discharge zones in the north central part. The highest hydraulic head is in the northern and northwest sections, with lowest in the southwest (Fig. 4). Most streams are structurally controlled.This result coincide with the work of [23],

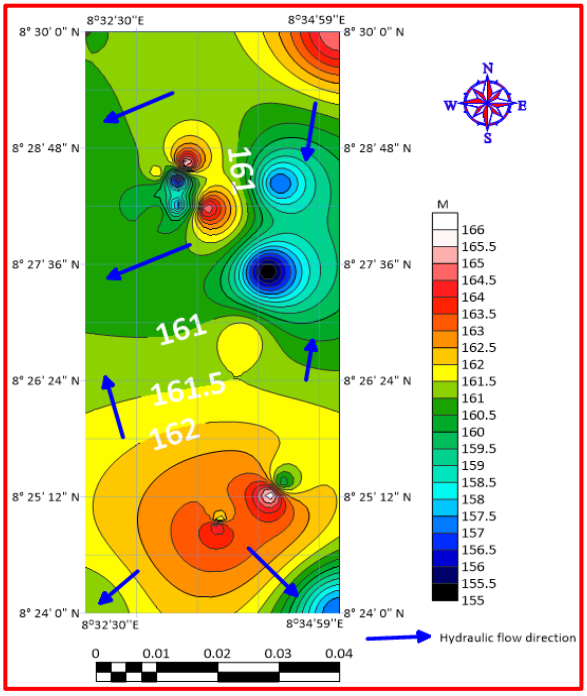

Figure 4: Groundwater flow direction map of the study area

Resistivity data interpretations

Smoothened data were inputed into a computer system using IP2WIN software to generate sounding curves. They were smoothened until smooth layer curves were obtained. The curve type varies from KH, QH, H, and Q-types (Fig. 5a-d). The percentage distribution of these curves were (11.12%) KH, (44.44%) represent QH, 22.22% represent H type and 22.22% were Q-types (Fig. 6). The results of the computer-iterated model, resistivity values, geoelectric layers, thickness and depths are presented in Table 1. The resistivity values obtained from computer iterated models varies with depth as reflected by different curve types. They resistivity values ranged from 1.28 to 2792 Ωm. Resistivity value that is less than 1.28 Ωm nearly in all VES stations suggests the subsurface geology is devoid of materials of low resistivity. Resistivity values from 29.3 to 104.5 Ωm were tie to top soil, resistivity of 1 to 500 Ωm at depth geologically tie to shale and resistivity of 500 Ωm and above as sand or sandstone. The shale horizon is common to almost all VES stations which confirms the sandy-shale nature of the area. Geologically attributable to moderate energy environment of deposition in the area. Its thickness may varies from 17.1 to 250 m in the area. The aquifer are confined by the shale layer except areas around VES stations 4, 8 and 9, where the aquifer is unconfined. The result is in agreement with the work of [24, 12].

Table 1: The results of the computer-iterated model, resistivity values, geoelectric layers, thickness and depths in the study area

VES Station	Coordinate	Parameters	Layer 1	Layer 2	Layer 3	Layer 4	Layer 5
1	N08° 28'09.5"	*P* (Ωm)	67.8	12.3	189	929	7039
	E08° 33' 40.9"	*h* (m)	8.3	41.2	13	37.5	Infinity
		d (m)	8.3	49.5	62.5	100	Infinity
		Interpretation	Top soil	Shaly sand	Shale	Sandstone	Sandstone
2	N08° 28' 11.4"	*P* (Ωm)	443	23.7	3.58	464	
	E08° 33' 42.2"	*h* (m)	1.67	9.8	177	Infinity	
		d (m)	1.67	12.8	128	Infinity	
		Interpretation	Top soil	Shaly sand	Shale	Shale	
3	N08° 28' 12.1"	*P* (Ωm)	106	10.2	4812	79.4	
	E08° 33' 32.9"	*h* (m)	3.22	50.8	21.1	Infinity	
		d (m)	3.22	54.1	75.1	Infinity	
		Interpretation	Top soil	Shale	Sandstone	Shale	
4	N08° 28' 12.7"	*P* (Ωm)	489	124	5.91	66.5	882
	E008° 33' 24.5"	*h* (m)	1.54	4.25	41.3	203	Infinity
		d (m)	1.54	5.79	47.1	250	Infinity
		Interpretation	Top soil	Shale	Shale	Shale	Sandstone
5	N08° 28' 18.4"	*P* (Ωm)	100	36.3	4.64	929	
	E08° 33' 9.9"	*h* (m)	2.68	9.51	9.3	Infinity	
		d (m)	2.63	12.2	109	Infinity	
		Interpretation	Top soil	Shale	Shale	Sandstone	
6	N08° 28' 38.5"	*P* (Ωm)	293	1.28	20.2	4.74	
	E08° 33' 29.5"	*h* (m)	5.97	5.85	5.24	Infinity	
		d (m)	5.97	11.8	17.1	Infinity	
		Interpretation	Top soil	Shale	Shale	Shale	
7	N08° 28' 32.6"	*P* (Ωm)	304	3.46	14.9	2526	
	E08° 33' 12.2"	*h* (m)	5.97	5.85	5.24	Infinity	
		d (m)	5.97	11.8	17.1	Infinity	
		Interpretation	Top soil	Shale	Shale	Sandstone	
8	N08° 28' 28.5"	*P* (Ωm)	59.1	5.88	126	1539	2792
	E08° 33' 24.4"	*h* (m)	3.69	24.5	10.3	87	infinity
		d (m)	3.69	28.2	38.5	126	infinity
		Interpretation	Top soil	Shale	Shale	Sandstone	Sandstone
9	N08° 28' 08.4"	*P* (Ωm)	62.9	3.66	25.5	4.23	47.6
	E08° 33' 12.1"	*h* (m)	6.45	8.44	1.37	172	infinity
		d (m)	6.45	14.9	16.3	189	infinity
		Interpretation	Top soil	Shale	Shale	Shale	Shale

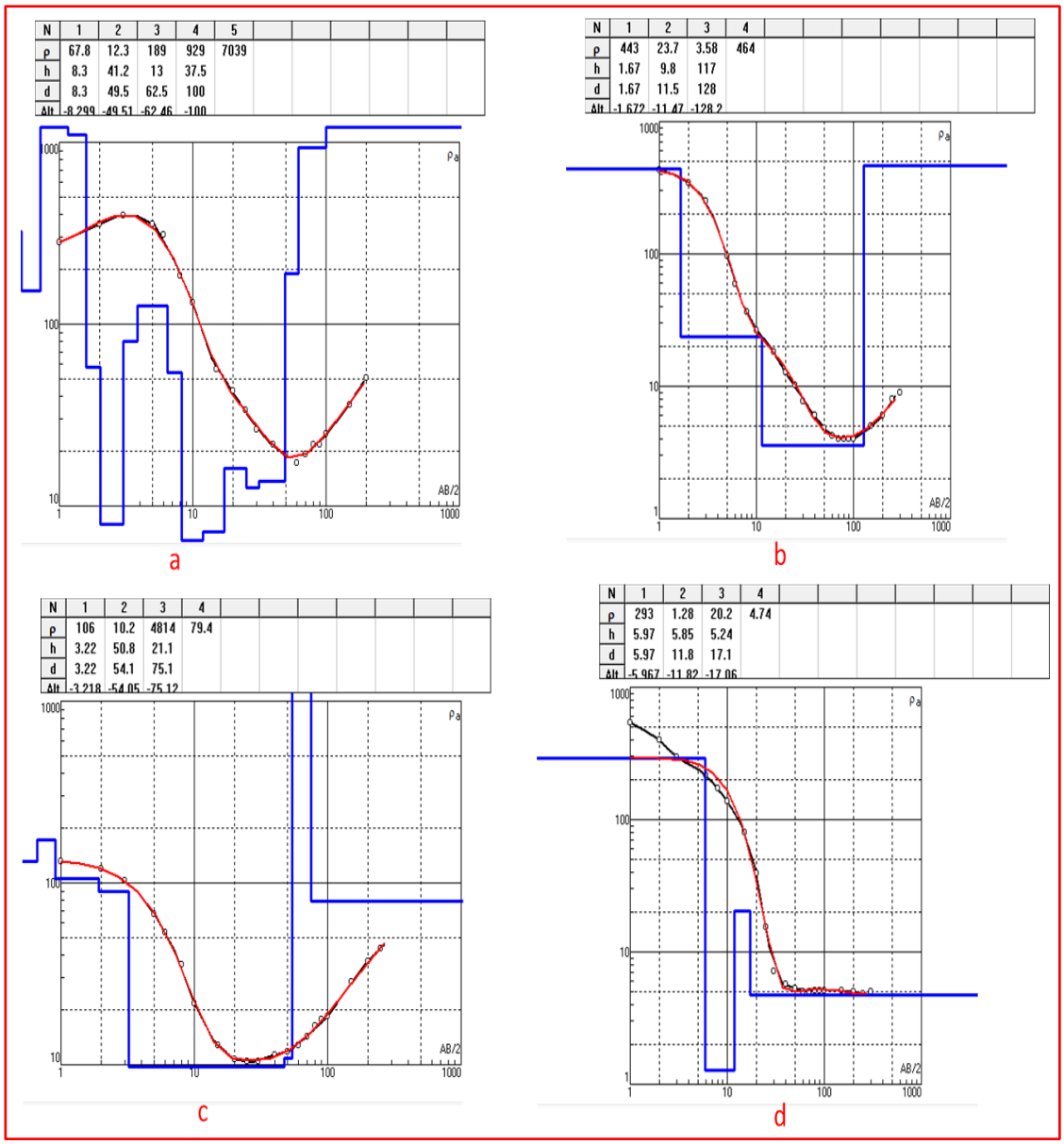

Figure 5(a, b, c & d): Curve types in the study area

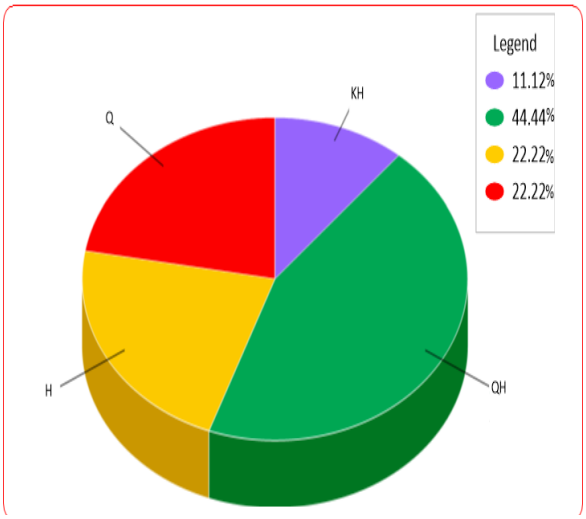

Figure 6: Distribution of curve types in the study area

Assessment of Groundwater Potential and Aquifer Protective Capacity in the area

The study area has overburden thicknesses ranging from 17.1 to 250 m, with an average thickness of 125 m. The study area is divided into four zones based on groundwater potentials (Fig. 7): Zone A, B, C, and D. The result coincides with the work of [23], a minimum overburden thickness of 25 m for viable groundwater abstraction.

The area's aquifer protective capacity, calculated using overburden thickness (Table 2), is excellent due to its combination of confined and unconfined aquifers, with the exception of VES 6 and 7 having the lowest capacity (Fig. 8). The result from the groundwater potentials and aquifer protective capacity is in line with the works of many researchers [14, 25, 26].

Table 2: Aquifer protective capacity rating [25]

S/N	Rating	Remark
1	>10	Excellent
2	5 – 10	Very good
3	0.2-4.9	Moderate
4	0.1 - 0.19	Weak
5	<0.1	Poor

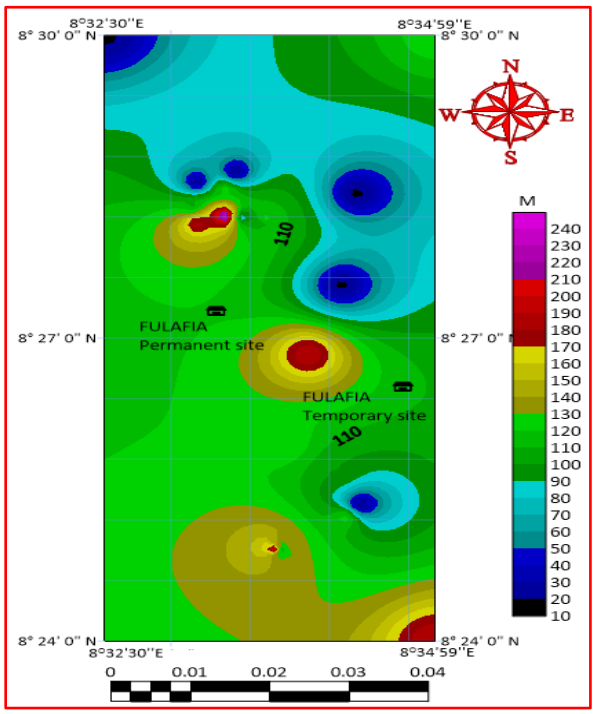

Figure 7: Groundwater potential map of the study area

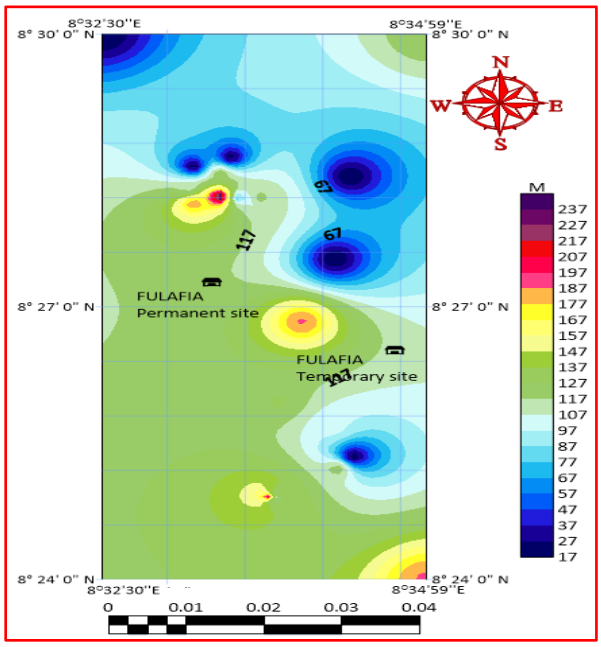

Figure 8: Aquifer protective capacity map of the study area

Groundwater quality assessment in the study area

Drinking suitability assessment

The analyzed groundwater samples are presented with physicochemical and descriptive statistics Table 3. The physicochemical parameters in drinking water align with WHO Standard [27], with low concentrations indicating natural processes like water-rock interactions, except for nitrate, which can cause unpleasant taste and scale deposits [28]. The samples show HCO_3^- concentrations below WHO's 2017 250 mg/L limit, while Ca^{2+} and Mg^{2+} concentrations range from 1.36 to 18.3 mg/L, with averages of 7.42 and 26.7 mg/L, respectively (Table 4). Crops grown on soils with a calcium and magnesium imbalance may display toxic symptoms [5].

The study area's groundwater has a Na^+ concentration ranging from 3.7 to 29.9 mg/L. 7.18 mg/L is the average value (Table 3). Additionally, K^+ levels vary from 1.1 to 2 mg/L. Every concentration of Na^+ and K^+ is within permissible bounds (Table 4). Iron chlorosis and magnesium deficiency in plants can be brought on by high K^+ concentrations. Although an imbalance between Mg^{2+} and K^+ can be harmful, high calcium levels can reduce the effect [29].

The values of SO_4^{2-} concentrations fall within the WHO's [27] permissible limit of 250 mg/L (Table 4). SO_4^{2-} salts disrupt the cationic balance in plants by reducing calcium uptake and increasing sodium and potassium adsorption, which impacts sensitive crops. The average Cl^- value is 15.87 mg/L, with a range of 7.89 to 39.8 mg/L. Moreover, NO_3^- concentrations vary between 11.1 and 55.9 mg/L. All concentrations of Cl^- and NO_3^- fall between the 250 and 50 mg/L, which is within the acceptable limits [27]. Except for sample 15 (Fig. 9), whose NO_3^- concentration was higher than the WHO's 2017 allowable limit (Table 4). In plants, NO_3^- is a necessary form of ingredient. Leguminous plants can fix it; it occurs in the soil. NO_3^- is thought to be a sign of contamination in public water supplies [7]. The result from the water quality analysis coincides with the work of [7, 28].

Table 3: Statistical summary of the physicochemical and calculated parameters in the study area

Sample Code	Coordinate	Ca^{2+}	Mg^{2+}	Na^{+}	K^{+}	HCO_3^-	SO_4^{2-}	Cl^-	NO_3^-
S1	N08 28' 14.2"E08 33' 09.2"	3.9	6	8.1	1.1	21	39	39.8	11.1
S2	N08 28' 16.3"E08 33' 08.0"	3.3	12.1	29.9	1.8	27	13	23.8	14.9
S3	N08 28' 17.8"E08 33' 06.8"	8.5	14.5	4.9	2	19	11	14.8	27.2
S4	N08 28' 17.2"E008 33' 06.1"	5.8	8.4	4.3	1.5	23	49	16.8	21.6
S5	N08 28' 22.2"E08 33' 05.7"	8.3	10.1	8.9	2	49	26	12.8	24.9
S6	N08 28' 18.8"E08 33' 09.9"	9.5	2.34	3.7	2	31	39	7.89	11.1
S7	N08 28' 18.0"E08 33' 19.5"	11.1	0.87	5.9	1.8	41	28	14.8	14.9
S8	N08 28' 12.9"E08 33' 23.5"	18.3	26.7	4.9	2	71	13	14.8	26.9
S9	N08 28' 08.0"E08 33' 30.6"	1.36	5.5	5.9	1.5	35	24	14.8	21.6
S10	N08 28' 12.8"E08 33' 31.0"	7.22	11.9	6.1	1.1	53	26	15.8	24.9
S11	N08 28' 12.9"E08 33' 46.3"	5.75	14.3	5.8	1.8	99	11	14.8	23.8
S12	N08 28' 25.4"E08 33' 30.6"	12.6	12.7	5.09	2	85	43	10.8	26.5
S13	N08 28' 24.3"E08 33' 22.2"	2.82	4.7	5.9	1.5	33	39	11.8	12.4
S14	N08 28' 12.5"E08 33' 29.0"	5.75	12.7	5.7	2	35	9	15.7	16.9
S15	N08 28' 22.8"E08 33' 26.7"	13.1	3.1	6	1.7	65	15	16.8	55.9
WHO [25]		75	50	200	200	50	250	250	50
	Min.	1.36	0.87	3.7	1.1	19	9	7.89	11.1
	Max.	18.3	26.7	29.9	2	99	49	39.8	55.9
	Mean	7.42	9.18	7.18	1.69	44.13	24.63	15.87	21.61
	Stand. Dev.	4.56	6.53	6.36	0.32	24.32	13.45	7.34	11.01

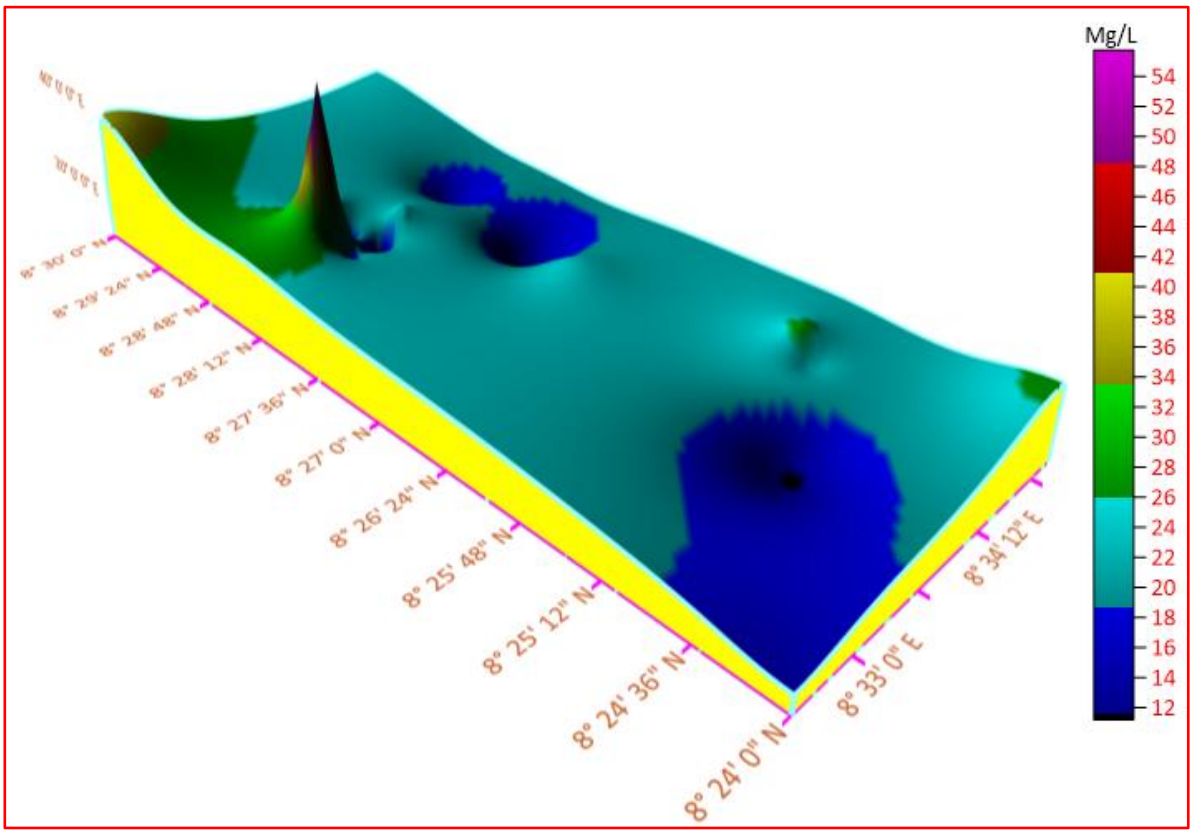

Figure 9: Nitrate concentration in the study area

Water quality index (WQI) in the area

The optimal values, unit weights, and standard values for the water quality variables are displayed in Table 4. The WQI states that the best water quality is indicated by a low number, while the worst quality is indicated by a higher number. Estimated WQI values in the area ranged from 3.11 to 10.14. The computed WQI values for the study area are displayed in Table 5. According to the Table 6 range, the WQI for each sample shows exceptionally high water quality [30].

Table 4: Ideal values and unit weights for water quality variables and their standard values

S/N	Parameter	WHO Standard	$\frac{1}{S} = wi$
1	Ca^{2+}	75	0.013
2	Mg^{2+}	50	0.020
3	Na^{+}	200	0.005
4	K^{+}	200	0.005
5	HCO_3^{-}	50	0.020
6	SO_4^{2-}	250	0.004
7	Cl^{-}	250	0.004
8	NO_3^{-}	50	0.020

Table 5: Computed water quality values for the study area

Sample ID	WQI Value	Water Type (Class)
1	4.63	Excellent water
2	3.11	Excellent water
3	4.41	Excellent water
4	4.38	Excellent water
5	5.63	Excellent water
6	10.14	Excellent water
7	3.74	Excellent water
8	6.44	Excellent water
9	3.37	Excellent water
10	7.08	Excellent water
11	7.91	Excellent water
12	5.73	Excellent water
13	3.14	Excellent water
14	3.54	Excellent water
15	7.17	Excellent water

Table 6: Water quality range as per WQI [30]

WQI	Water Types (Class)
0-50	Excellent
50–100	Good
101–200	Poor water
201–300	Very poor
>300	Unsuitable

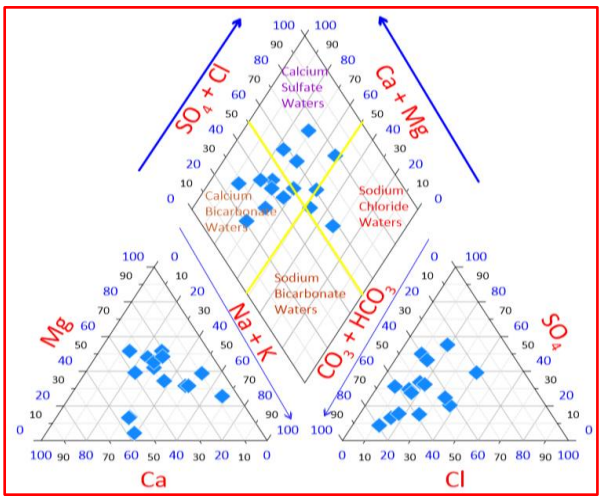

Figure 10: Groundwater classification in the study area

Groundwater classification in the study area

The study area's waters were classified using chemical parameters like anionic and cationic concentrations, using a Piper diagram to identify similarities and dissimilarities [31]. Piper diagram shows groundwater samples with varying ion properties, with seven classified under calcium bicarbonates, five under calcium sulfate, and two under sodium chloride waters (Fig. 10). The work is consistent with that of [7] within the Lafia sandstone aquifers. Industries can generally use water with this composition as long as the total dissolved solids stay within acceptable bounds [7].

Irrigational water quality of the study area

Sodium adsorption ratio (SAR)

The study area's groundwaters are classified as excellent for irrigation based on SAR values (Table 7). Groundwater with a SAR value below 10 meq/L is considered excellent, while those between 10 and 18 meq/L are considered good [30, 31]. Calcium and magnesium, when present in sufficient amounts, can counteract the effects of sodium and enhance soil properties. High sodium content in irrigation water poses a significant risk to soil due to its impact on its structure [29]. This finding is in line with the work of [29].

Table 7: Calculated groundwater parameters for domestic and irrigation used in the study area

Sample Code	SAR	KR	MAR	CAI
S1	3.07	0.54	60.61	0.77
S2	6.54	1.20	78.57	0.08
S3	1.01	0.17	62.72	0.59
S4	1.36	0.30	59.15	0.65
S5	2.07	0.48	54.89	0.15
S6	1.14	0.31	19.76	0.28
S7	2.41	0.49	7.27	0.48
S8	0.87	0.11	59.33	0.48
S9	3.20	0.86	80.17	0.50
S10	1.97	0.32	62.24	0.54
S11	1.61	0.29	70.27	0.48
S12	1.17	0.20	60.20	0.27
S13	2.60	0.78	62.50	0.37
S14	1.64	0.31	68.83	0.51
S15	1.55	0.37	19.14	0.54
Mini	0.87	0.11	7.27	0.08
Max	6.56	55.9	78.57	0.77
Mean	2.14	21.61	55.04	0.45
Stand. Dev	1.18	11.01	30.30	0.25

Kelly's ratio (KR)

From this study, all the groundwater samples have Kelly Ratio of less than 1($KR < 1$) except sample number 2 with ($KR > 1$) which makes the water unfit for irrigation (Table 7), which is in agreement with the work of [22]. Kelly's ratio (KR) introduced by [22] is an important parameter used in the evaluation of water quality for irrigation. This parameter is based on Na, Ca and Mg levels in the groundwater. According to this

classification, groundwater with a KR value greater than one (KR > 1) is deemed unfit for irrigation.

Magnesium adsorption ratio (MAR)

In contrast to samples 6, 7, and 15, which are below 50% and thus appropriate for irrigation in the region, MAR results from this study indicate that all of the samples 1, 2, 3, 4, 5, 8, 9, 10, 11, 12, 13, and 14 are above 50%, which has a negative impact on crop yield as the soil becomes more alkaline (Table 7). In most waters, calcium and magnesium keep things in balance. [21] contends that as the soil becomes more alkaline, a high magnesium hazard value (50%) has a negative impact on crop yield. [29] MAR results, in contrast, indicate that all of the samples were below 50% and, therefore, appropriate for irrigation.

Chloro-alkaline indices (CAI)

Ion exchange between groundwater ions and their host rock is indicated by CAI. An exchange between Na + K and Ca and Mg is indicated by a negative CAI value. A positive CAI value would be noted if these parameters did not exchange. There is no exchange between Na and K in waters with Ca and Mg in the host rocks within the study area, as indicated by the positive CAI values recorded by all of the ground waters in the area (Table 7). The outcome is consistent with the findings of [31].

Conclusion

The paper revealed groundwater potentials at the Federal University of Lafia, Nigeria and its suitability for drinking and irrigation. The area's aquifer system, primarily composed of sandy-shale with resistivity values ranging from 0 – 1600 Ωm and overburden thickness from 17.1 to 250 m. The groundwater potential is moderate to high; the aquifer protective capacity (APC) is excellent due to the low resistivity and high thickness of the overburden shale layer. The WQI for all samples in the area indicate excellent water quality and is suitable for drinkingAll samples have Kelly ratio of less than 1 (KR<1), except for sample number 2, which has a KR > 1, rendering the water unsuitable for irrigation. According to MAR, samples 1, 2, 3, 4, 5, 8, 9, 10, 11, 12, 13, and 14 are above 50%, indicating a negative impact on crop yield as the soil becomes more alkaline. Samples 6, 7, and 15 are below 50%, indicating that the area is suitable for irrigation. All samples have positive CAI values, which suggests that there is no exchange of Na and K in the waters with Ca and Mg in the host rocks in the study area. These findings have far-reaching implications as policy-makers and stakeholders should incorporate groundwater sustainable practices and their suitability into development strategies. Furthermore, by emphasizing the advantages of portable, safe drinking water for economic planning, the study adds to the body of existing literature. This study admits its shortcomings, including the uncertainty in interpreting geophysical data and the detection limits of certain geochemical instruments. To lower uncertainties and produce more accurate results, future studies in the field should concentrate on integrating geochemical models and their isotopic sources. In all, access to safe water is essential for survival, and its availability or contamination can have detrimental effects on public health, resulting in illnesses or even epidemics.

Conflict of interest: The authors declare no conflict of interest.

References

[1] Umar, N. D., Igwe, O. & Idris, I. G. (2019). Evaluation and characterization of groundwater of the Maastrichtian Lafia formation, Central Benue trough, Nigeria. *Journal of Earth System Science*, 128(6), 168. https://doi.org/10.1007/s12040-019-1199-1

[2] Raghunath, H. M. (2010). *Groundwater*. New Age International Publ. New Delhi.

[3] Araffa, S. A. S., Soliman, S. A., El-Khafif, A., Younis, A. & Shazley, T. F. (2019). Environmental investigation using geophysical data at East Sadat City, Egypt. *Egyptian Journal of Petroleum*, 2, 117-125. https://doi.org/10.1016/j.ejpe.2018.12.002.

[4] Monde, M. J., Olugun, S. & Abubakar, M. I. (2021). Adudu and its environment groundwater potential assessment, Akiri, Sheet 232, Middle Benue Trough, Central Nigeria. *Mazedan Journal of Civil Engineering & Architecture*, 1(1), 22–28.

[5] Wubon, J. R. & Kana, A. A. (2019). Aspects of the geology and hydrogeology around Awe Town, Nigeria. *International Journal of Coal, Geology and Mining Research*, 1, 36–50. http://www.eajournals.org/

[6] Binbol, N. L. (2006). *A climate of Nasarawa state: Report of Geographical Prospective on Nasarawa State*. Department of Geography, Nasarawa State University. https://doi.org/10.3354/cr032247

[7] Offodile, M. E. (2002). Groundwater study and development in Nigeria. *Mecon. Services Ltd., Jos, Nigeria*, 5, 494–502.

[8] Mohammed, S. C. & Ali, M. (2019). Hydrogeochemistry of the Middle Benue Trough, Nigeria. *Journal of Water Resources and Ocean Science*, *7*(5), 70-76. https://doi.org/10.11648/j.wros.20180705.11

[9] Nwajide, C. S. (1990). Cretaceous sedimentation and paleogeography of the central Benue Trough: The Benue trough structure and evolution. *International Monograph Series, Braunschweig*, 19-38.

[10] Andarawus, Y., Nur, A., Musa N., Adamu, A. & Mu'awiya, B. A. (2022a). Geoelectric investigation for aquifer characterization in boi and environs, Bauchi State, Northeast, Nigeria. *Dutse J. of Pure & Appl. Sci*., 8(2a), 149-170. https://dx.doi.org/10.4314/dujopas.v8i2a.16

[11] Knödel, K., Lange, G. & Voigt, H. (2007). *Environmental Geology*. (A handbook of field methods and case studies). Springer, 1374p.

[12] Umar, N. D. & Igwe, O. (2019). Geo-electric method applied to groundwater protection of a granular sandstone aquifer. *Applied Water Science,* 9, 112. https://doi.org/10.1007/s13201-019-0980-2

[13] Zohdy, A. A., Eaton, G. P. & Mabey, D. R. (1974). *Application of Surface Geophysics to Ground-Water Investigations*. 1st Edn., Chapter Book 2, USGS Publication, USA., p. 116.

[14] Yohanna, A., Umar, N. D., Jabbo, J. N., Galumje, S. S. & Aliyu, A. I. (2022a). Preliminary geological investigation into the causes of foundation failure in Jalingo, Northeast Nigeria. *Science Forum* (*Journal of Pure and Applied Sciences*), 22, 432–443. http://dx.doi.org/10.5455/sf.10603

[15] Yisa J & Jimoh T. (2010). Analytical studies on water quality index of river Landzu. *American Journal of Apply Science*, 7, 453–458. https://doi.or/10.3844/ajassp

[16] Tyagi, S., Singh, P., Sharma, B. & Singh, R. (2014). Assessment of water quality for drinking purpose in District Pauri of Uttarkhand, India. *Appl. Ecol. Environ. Sci.,* 2(4), 94–99.

[17] USSL (US Salinity Laboratory) (1954). *Diagnosis and Improvement of Saline and Alkaline Soils*. Agriculture Handbook No. 60 USDA, p 160.

[18] Ayers, R. S. & Westcott, D. W. (1985). *Water Quality for Agriculture* (No. 29). Food and Agriculture Organization of the United Nations, Rome, Italy

[19] Michael, A. M. (1992). *Irrigation Theory and Practices*. Vikash Publishing House Pvt. Ltd., New Delhi, pp 686–740.

[20] Richards, L. A. (1954). Diagnosis & improvement of saline alkali soils: Agriculture, handbook. US Department of Agriculture, Washington DC, vol. 160, p 60.

[21] Raghunath, H. M. (1987). *Groundwater*. Wiley Eastern Ltd., New Delhi, pp. 344–369.

[22] Kelly, W. P. (1963). Use of saline irrigation water. *Soil Sci.,* 95, 355–390.

[23] Yohanna, A., Musa, N., Balogun, F. O., Jabbo, J. N., Adamu, A. & Galumje, S. S. (2022b). Assessment of groundwater potentials of crystalline basement complex aquifers using hydraulic properties in the Ussa Area of Taraba State, North-east Nigeria. *FUDMA Journal of Sciences* (FJS) , 6(3), 88–94. https://doi.org/10.33003/f js-2022-0603-974

[24] Olurunfemi, M. O. & Okakune, E. T. (1992). Hydrogeological and geological significance of geoelectrical survey of Ile-Ife, Nigeria. *Journal of Mining and Geology,* 28, 221-222.

[25] Olusegun, O. A., Adeolu, O. O. & Dolapo, F. A. (2016). Geophysical investigation for groundwater potential and aquifer protective capacity around Osun State University (UniOsun) College of Health Sciences. *Am. J. Water Resour.,* 4(6), 137–143.

[26] Aina, J. O., Adeleke, O. O., Makinde, V., Egunjobi, H. A. & Biere, P. E. (2019). Assessment of hydrogeological potential and aquifer protective capacity of Odeda, Southwestern Nigeria. *RMZ–M&G*, 66, 199–210.

[27] WHO (2017). *Guidelines for Drinking Water Quality*. Fourth edition incorporating the first addendum. World Health Organizaion, Geneva, Switzerland.

[28] Yohanna, A., Musa, N., Balogun, F. O., Agada E. A., Adamu, A. & Galumje, S. S. (2022c). Investigation of groundwater contamination in some selected areas of Bogoro and Environs, north-east Nigeria. *FUDMA Journal of Sciences* (FJS), 6(1), 358–367. https://doi.org/10.33003/f js-2022-0603-974

[29] Musah, S., Felix, A., Michael, S. H., Dickson, A. & Enoch, A. (2017). Evaluating the suitability of groundwater for irrigational purposes in some selected districts of the Upper West region of Ghana. *Appl. Water Sci*., 7, 653–662. DOI: 10.1007/s13201-015-0277-z

[30] Akter, T., Jhohura, F. T., Akter, F., Chowdhury, T. R., Mistry, S. K., Dey, D., Barua, M. K., Islam, M. A. & Rahman, M. (2016). Water quality index for measuring drinking water quality in rural Bangladesh: A cross-sectional study. *J. of Health, Population and Nutrition,* 35, 4.

[31] Piper, A. M. (1994). A graphic procedure in geochemical interpretation of water analysis. *Trans. Am. Geophys Union,* 25, 914–923.

Citing this Article

Umar, N. D., Yohanna, A., Aliyu, I. A., Usman, A. S., Aliyu, S., Musa, S. T. & Idris, M. S. (2025). Groundwater potential and its suitability for drinking and irrigation purposes in Federal University of Lafia, Nasarawa State, North-Central Nigeria. *Lafia Journal of Scientific and Industrial Research, 3*(2), 59–70. https://doi.org/10.62050/ljsir2025.v3n2.538